

Article

# Synthesis and Investigation of Properties of Beryllium Ceramics Modified with Titanium Dioxide Nanoparticles

Alexandr Pavlov<sup>1</sup>, Zhuldyz Sagdoldina<sup>1</sup>, Almira Zhilkashinova<sup>2</sup> , Nurtoleu Magazov<sup>1,3,\*</sup> , Zhangabay Turar<sup>1</sup> and Sergey Gert<sup>3</sup>

<sup>1</sup> Surface Engineering and Tribology Research Center, Sarsen Amanzholov East-Kazakhstan University, Ust-Kamenogorsk 070000, Kazakhstan

<sup>2</sup> National Laboratory of Collective Use, Sarsen Amanzholov East-Kazakhstan University, Ust-Kamenogorsk 070000, Kazakhstan

<sup>3</sup> Center of Excellence “VERITAS”, Daulet Serikbayev East Kazakhstan Technical University, Ust-Kamenogorsk 070000, Kazakhstan

\* Correspondence: magazovn@gmail.com; Tel.: +7-747-426-30-19

**Abstract:** Samples of beryllium ceramics, with the addition of micro- and nanoparticles TiO<sub>2</sub>, have been obtained by the method of thermoplastic slip casting. The microstructure of batch ceramics, consisting of micropowders and ceramics with TiO<sub>2</sub> nanoparticles sintered at an elevated temperature, has been investigated. It was found that the introduction of TiO<sub>2</sub> nanoparticles leads to changes in the mechanisms of mass transfer and microstructure formation, and the mobility of TiO<sub>2</sub> at interfacial grain boundaries increases, which leads to the formation of elements of a zonal shell structure. The reduction of intergranular boundaries leads to an increase in density, hardness, and mechanical strength of ceramics. The whole complex of properties of the synthesized material, with the addition of TiO<sub>2</sub> nanoparticles in the amount of 1.0–1.5 wt.%, leads to an increase in the ability to absorb electromagnetic radiation in the frequency range of electric current 8.2–12.4 GHz. The analysis and updating of knowledge on synthesis, and the investigation of properties of beryllium ceramics modified by nanoparticles, seems to be significant. The obtained results can be used in the creation of absorbers of scattered microwave radiation based on (BeO + TiO<sub>2</sub>) ceramics.

**Keywords:** beryllium oxide; TiO<sub>2</sub> nanoparticles; microstructure; apparent density; microhardness; microwave radiation; reflection losses



**Citation:** Pavlov, A.; Sagdoldina, Z.; Zhilkashinova, A.; Magazov, N.; Turar, Z.; Gert, S. Synthesis and Investigation of Properties of Beryllium Ceramics Modified with Titanium Dioxide Nanoparticles. *Materials* **2023**, *16*, 6507. <https://doi.org/10.3390/ma16196507>

Academic Editor: Lidija Ćurković

Received: 9 August 2023

Revised: 17 September 2023

Accepted: 28 September 2023

Published: 30 September 2023



**Copyright:** © 2023 by the authors. Licensee MDPI, Basel, Switzerland. This article is an open access article distributed under the terms and conditions of the Creative Commons Attribution (CC BY) license (<https://creativecommons.org/licenses/by/4.0/>).

## 1. Introduction

Presently, vacuum-dense ceramic materials that weaken microwave radiation in a wide frequency range are of particular interest in the development of modern electronic devices [1]. Such materials have the ability to absorb electromagnetic waves in certain frequency ranges and convert them into thermal energy [2]. The rapid development of vacuum electronic devices operating in extreme environments [3] requires microwave attenuation materials to have high thermal conductivity, fine grain structure, and mechanical strength, in addition to excellent microwave absorption capability. All these are necessary to prevent damage to electronic devices operating in corrosive environments [4]. Of all the known composite materials that meet the stated requirements, beryllium oxide [5] is the most promising due to its outstanding characteristics such as high thermal conductivity, good mechanical properties, high temperature stability, and moderate dielectric constant [6]. The unique combination of physical and chemical properties of beryllium oxide [7] determines a wide range of its use in various fields of modern engineering and special instrumentation [8]. High radiation resistance of BeO ceramics [9], thermal conductivity, dielectric strength, and transparency to X-ray, UV, IR and microwave radiation make BeO ceramics a promising material for use in a variety of devices and instruments of electronic technology for critical applications [10]. Pure BeO ceramics has high thermal conductivity, about

280–320 W/(m·K) and increased electrical resistance ( $\sim 1 \times 10^{15}$  Ohm·cm) [11], comparable to the thermal conductivity of chemically pure copper ( $\sim 400$  W/(m·K)) [12].

Various additives in the composition of BeO ceramics can lead to the presence of developed interfaces and intergranular interactions that affect the physicochemical and performance characteristics of composite ceramics. Titanium dioxide is one of such additives that can significantly change the conductive and other properties of BeO ceramics used as bulk electromagnetic energy absorbers [13].

The available data on the BeO–TiO<sub>2</sub> system are contradictory, and the question of the existence of any beryllium titanates remains open. Thus, according to the authors [14], the results of the study of electrically conductive ceramics from the BeO:TiO<sub>2</sub> mixture show that the two oxides involved create independent substructures in the mixed ceramics. The TiO<sub>2</sub> substructure provides the electrical conductivity of the composite ceramic. The system is free of compounds; a single eutectic exists at a TiO<sub>2</sub> content of about 85 wt.% and a temperature of 1670 °C. Currently, BeO is not known to form any “titanates” when interacting with TiO<sub>2</sub> [15]. However, in paper [16] using the density functional theory, the structural, thermodynamic, and optoelectronic behavior of BeTiO<sub>3</sub> perovskite in the pressure range 0–160 GPa was modeled. It was found that the studied perovskite is thermodynamically stabilized in the cubic phase, along with structural and mechanical properties.

It is known that the addition of TiO<sub>2</sub> microparticles to the composition of BeO-based ceramics, with appropriate heat treatment in a weakly reducing environment of carbon monoxide, leads to the appearance of electrically conductive and dielectric properties of ceramics [17]. The main advantage of (BeO + TiO<sub>2</sub>) ceramics is the thermodynamic stability of properties, high mechanical strength, thermal conductivity, and excellent absorption characteristics [18]. It was found that the addition of 30 wt.% TiO<sub>2</sub> to BeO ceramics leads to a significant increase in the dielectric constant and the degree of TiO<sub>2</sub> reduction, which is accompanied by an increase in the dielectric loss angle tangent [19].

It was first reported in [20] about obtaining the material of BeO + TiO<sub>2</sub> composition. It is known that the addition of TiO<sub>2</sub> to BeO ceramics after sintering, under the same thermodynamic conditions in the amount from 5 to 40 wt.%, is accompanied by an increase in density, dielectric constant, and other properties [21].

At present, the composition BeO + 30 wt.% TiO<sub>2</sub> ( $\mu\text{m}$ ) is a commercially available microwave ceramic under the brand name BT-30.

The attenuation coefficient of microwave radiation passing through (BeO + TiO<sub>2</sub>) ceramics in the frequency range of 8.5–12 GHz is 19–20 dB. Titanium in relation to BeO has relatively low solubility  $10^{-3}$ – $10^{-4}$  at. % and forms many oxides: TiO<sub>2</sub>, Ti<sub>2</sub>O<sub>3</sub>, Ti<sub>3</sub>O<sub>5</sub> and others [22].

When such ceramics are heated in the temperature range from 750 to 1000 °C in hydrogen, TiO<sub>2</sub> is transformed into the compound Ti<sub>2</sub>O<sub>3</sub>. Under the action of temperature 2000 °C in hydrogen medium under pressure 13–15 MPa, TiO<sub>2</sub> is reduced to TiO. In the reducing environment of carbon monoxide under the action of temperature, the reaction  $\text{TiO}_2 + \text{C} \rightarrow \text{TiO} + \text{CO}$  takes place [23]. During thermal treatment of (BeO + TiO<sub>2</sub>) ceramics in the atmosphere of carbon monoxide, carbon penetrates into its internal structure [24]. In turn, in the process of sintering (BeO + TiO<sub>2</sub>) ceramics in the atmosphere of carbon monoxide, carbon residues in the billets, carbon from the graphite heater, and graphite grits, reducing gas CO, and interacting with TiO<sub>2</sub> leads to the replacement of part of the oxygen vacancies in the anionic sublattice of TiO<sub>2</sub> [25]. The process of isomorphic substitution of titanium ions and introduction of carbon ions into the inter-nodes of the TiO<sub>2</sub> crystal lattice is also observed [26].

Therefore, the electrical conductivity of (BeO + TiO<sub>2</sub>) ceramics is primarily affected by the carbon impurity. Thus, if there will be insufficient oxygen in the furnace atmosphere during sintering of (BeO + TiO<sub>2</sub>) ceramics, the reactions of its substitution by carbon ions are preferable and, consequently, the formation of oxygen vacancies in the structure of TiO<sub>2</sub>. In the case of an excess of oxygen in the furnace atmosphere during sintering, the most

probable reactions are the introduction of carbon into the inter-nodes and the substitution of titanium by carbon ions.

Thus, in the process of  $\text{TiO}_2$  reduction, when the oxidation degree changes in the series  $\text{Ti}^{4+} \rightarrow \text{Ti}^{3+} \rightarrow \text{Ti}^{2+}$ , the number of d-electrons increases. The reduction leads to partial occupancy of a narrow, weakly conducting 3d-zone, which is vacant in stoichiometric  $\text{TiO}_2$  [27]. The partially reduced  $\text{TiO}_2$  is a semiconductor with an electronic type of conductivity [28]. According to the studies carried out in [29], it was found that oxygen ion vacancies are the defects of rutile, and in [30] it is shown that it is titanium ions that are the defects of rutile, with  $\text{TiO}_2 \leftrightarrow \text{Ti}^{n+} + n\text{e}^- + \text{O}_2$ . It is assumed that titanium ions are located in the interstitials of the crystal lattice. The calculation of the electronic structure of  $\text{TiO}_2$  shows that instead of Ti and O ions, the introduction of carbon is energetically favorable [31]. Thus, the possibility to regulate the process of carbon introduction allows for control of the values of electrical conductivity of ( $\text{BeO} + \text{TiO}_2$ ) ceramics and to influence its ability to absorb electromagnetic radiation [32].

The authors of the present study found that the improvement of the electrophysical properties of such ceramics can be achieved by introducing  $\text{TiO}_2$  nanoparticles into its composition [33], which will contribute to the expansion of the operating frequency range, increase the stability of parameters during operation and exposure to external factors, and expand the technical characteristics in the field of special instrumentation. The authors also found that when the content of nanoparticles increases above 2.0 wt.% the viscosity of the slurry increases significantly, and it is not possible to mold the workpiece by the slurry casting method.

The main properties of  $\text{TiO}_2$  nanoparticles that contribute to the structural and electrophysical properties of such ceramics include the fact that with a decrease in the size of  $\text{TiO}_2$  particles, the absorption of electromagnetic energy occurs with the entire volume of the particle [34]. The physical processes occur during the sintering of ceramics based on BeO with the content of micro- and nanoparticles  $\text{TiO}_2$ . New regularities of mass transfer and microstructure formation during sintering of the system ( $\text{BeO} + \text{TiO}_2$ ) modified by  $\text{TiO}_2$  nanoparticles emerge. This occurs due to an increase in the diffusion mobility of  $\text{TiO}_2$  at the interfacial boundaries of microcrystals, which leads to a decrease in porosity and an increase in the physical and mechanical properties of ceramics. Nanocrystalline addition leads to an increase in the number of active centers, bulk and surface defects available for reactions. The reduction reactions proceed more efficiently and the electrical and chemical properties of the synthesized material are changed [35]. At present, the current production of beryllium oxide ceramics is established in the USA, China and Kazakhstan, so the analysis and updating of knowledge on the study of the properties of nanostructured ceramics using this strategically important material seems to be very significant. Thus, the goal of this study is to obtain prototypes of commercially available ceramics, composition:  $\text{BeO} + 30 \text{ wt.}\% \text{ TiO}_2$  with the addition of nanoparticles of titanium dioxide to study the structure, physical and mechanical properties and the ability of the synthesized material to absorb electromagnetic radiation. Maintaining the mass ratio of components will make it possible to trace the change in the properties of ceramics in comparison with the serial sample, which meets the requirements of the standards of the radioelectronic industry.

## 2. Materials and Methods

Experimental samples were prepared on the basis of micropowders of beryllium oxide with purity 99.9 wt.%, titanium dioxide with purity 99.5 wt.%, and nanopowders of titanium dioxide. The method of obtaining this is based on low temperature combustion of purified  $\text{TiCl}_4$  in the vapor phase in the presence of a catalyst. In this method of preparation, the morphology of the nanoparticles is crystals of a predominantly elongated shape, with a size of 50–80 nm, a diameter of 10–15 nm, and purity 99.9 wt.%. The particle sizes and surface morphology of the powders used are shown in Figure 1.

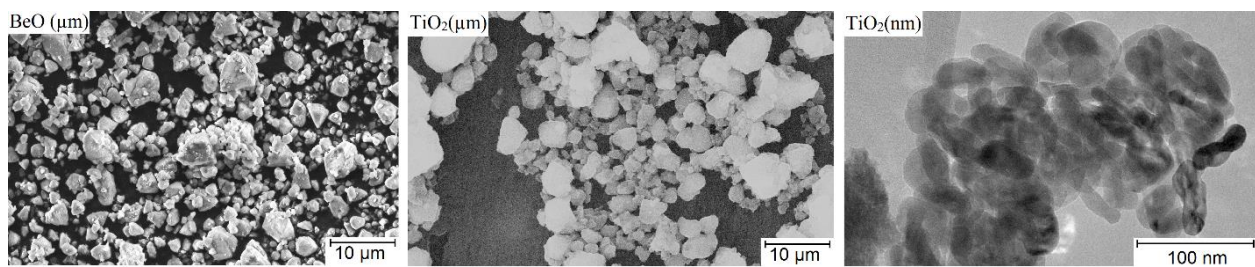


**Figure 1.** Electron image of beryllium oxide powder microparticles, titanium dioxide microparticles and nanoparticles.

Introduction of nanoparticles into the micron matrix of BeO and TiO<sub>2</sub> powders was carried out using an impeller-type reactor, the working body of which was filled with a liquid electrically nonconductive substance that does not react chemically with the particle material. Micro- and finely dispersed powders were loaded in the ratio of dry fraction to liquid fraction 1:7. The device of the reactor allows mixing of the charge components in the horizontal direction due to the rotation of blades, and the movement of flows in the liquid in the vertical direction occurs under the action of compressed air pressure supplied to the bottom of the reactor, providing effective distribution of TiO<sub>2</sub> nanoparticles throughout the volume of the charge.

Further, a thermoplastic slurry based on a wax–paraffin bond was prepared. The billet was molded on a casting machine for molding thermoplastic slurries into a collapsible mold. Firing of the binder from the billet was carried out in a muffle furnace at 1200 °C in aluminum oxide powder backfill. Sintering of the billet was carried out in a vacuum furnace with a graphite heater, packing the billet in a crucible made of beryllium oxide. The inside of the crucible was lined with molybdenum sheet. After laying the billets, the crucible was closed with a beryllium lid with technological holes for saturation of the billet with reducing gas CO. Sintering of the billet was carried out at 1660 °C with a holding time of 1 h. All experimental samples were obtained under the same regime, and saturation of the billet with reducing gas CO for all samples was made under the same conditions.

Thus, a series of experimental samples were obtained with the addition of TiO<sub>2</sub> nanoparticles according to Table 1.

**Table 1.** Compositions of the studied samples.

No. of Batch	Component Content, wt.%		
	BeO	TiO <sub>2</sub> (μm)	TiO <sub>2</sub> (Nano)
P0	70	30	-
P1	70	29.5	0.5
P2	70	29.0	1.0
P3	70	28.5	1.5

The sample of P0 composition is a serial sample of absorbing ceramics without the addition of nanoparticles.

Microstructure, particle size distribution and phase analysis of powders and sintered samples were studied on a scanning electron microscope JSM-6390LV, 2007 (JEOL Ltd., Tokyo, Japan), with a resolution in a high vacuum up to 3 nm and the possibility of imaging in secondary and reflected electrons. The magnification of the microscope ranged from 5× to 300,000× at accelerating voltages from 0.5 to 30 kV. Some photographs of the microstructure were also obtained on a Hitachi SU3500 scanning electron microscope (Hitachi, Tokyo, Japan). The magnification of the microscope is from 5× to 300,000× at accelerating voltages from 0.3 to 30 kV.

The study of phase composition of synthesized ceramics was carried out by X-ray diffraction and implemented using a powder X-ray diffractometer D8 Advance ECO (Bruker, Berlin, Germany). The diffractograms were taken in Bragg–Brentano geometry in the angular range  $2\theta = 20\text{--}90^\circ$ , with a step of  $0.05^\circ$  and a spectral acquisition time of 1.5 s at the point. To analyze the obtained diffractograms, as well as to determine the phase composition and structural parameters, we used the software Diffraction v. 4.2. The PDF-2 database was used to refine the phases.

Analyses to determine the values of apparent density were carried out according to the method described in GOST 2409-95 “Refractories. Method of determination of apparent density, open, total and closed porosity, water absorption”.

Determination of microhardness of the samples was carried out using the indentation method with the Vickers method. Diamond pyramid was used as an indenter, pressure force—500 N.

Mechanical strength was measured according to GOST 24409-80 “Ceramic electrotechnical materials”.

The particle size distribution and other studies of the ceramic microstructure were carried out using a BX-51 optical microscope (Olympus Corporation, Tokyo, Japan) with a digital camera and SIAMS 800 image analysis software.

Reflection coefficient values (S11/S22 Lin Mag) were measured using Keysight Technologies “Vector network analyzer P9373A” (Keysight Technologies, Santa Rosa, CA, USA) in the frequency range of 8.2–12.4 GHz.

To obtain reliable data, at least ten samples from each batch were measured. If the sample had defects in the form of cracks, shells and pores, such a sample was excluded from the experiment.

### 3. Results and Discussion

Beryllium oxide in relation to  $\text{TiO}_2$  is an inert compound, i.e., there is no chemical interaction potential between them. It is known that the solubility of Ti in BeO varies at the level of  $10^{-3}\text{--}10^{-4}$  at.%. The system  $\text{TiO}_2\text{--BeO}$  belongs to simple eutectic. In the literature there is information only about the presence of a region of solid solutions extending from 85 to 100 wt.%  $\text{TiO}_2$ , formed during melting in an oxygen–hydrogen flame [36].

On the phase diagram of  $\text{TiO}_2\text{--BeO}$  [36] above the temperature of  $1670^\circ\text{C}$ , titanium dioxide passes into the liquid phase. Therefore, in order not to “lose” mechanical properties due to crystal growth, the sintering temperature of ( $\text{BeO} + \text{TiO}_2$ ) ceramics should not be higher than  $1670^\circ\text{C}$ . Depending on the sintering mechanism, the microstructure of ceramics is also determined. In the case of the solid-phase sintering process, grains are formed by the processes of pore dissolution and growth of individual crystals.

The data of entropy calculation of equilibrium constants allow us to identify four main chemical reactions that can occur at a temperature of  $1660^\circ\text{C}$ , as shown in Table 2.

**Table 2.** Calculation of Gibbs energy change, which determines the possibility of spontaneous reaction at  $T = 1660^\circ\text{C}$ .

Chemical Reaction	$\Delta G$ , kJ/mol
$\text{TiO}_2 + \text{C} \rightarrow \text{TiO} + \text{CO}$	$\Delta G_T < 0$
$2\text{TiO}_2 + \text{C} \rightarrow \text{Ti}_2\text{O}_3 + \text{CO}$	
$3\text{TiO}_2 + \text{H}_2 \rightarrow \text{Ti}_3\text{O}_5 + \text{H}_2\text{O}$	
$\text{TiO}_2 + \text{CH} \rightarrow \text{CO}_2 + \text{TiH}$	

According to the results of the calculation of possible electrically conductive phases responsible for the conductivity of ceramics composition ( $\text{BeO} + \text{TiO}_2^{\mu\text{m}} + \text{TiO}_2^{\text{nano}}$ ) sintered at  $T = 1660^\circ\text{C}$ , the main electrically conductive phases are TiO,  $\text{Ti}_2\text{O}_3$ ,  $\text{Ti}_3\text{O}_5$ , and TiH. It is known that the compound  $\text{Ti}_2\text{O}_3$  when fused with  $\text{TiO}_2$  under the influence of temperature (according to different data, at  $1600\text{--}2000^\circ\text{C}$ ) forms a phase based on  $\text{Ti}_3\text{O}_5$ , which is a double oxide of tri- and tetravalent titanium:  $\text{Ti}_2^{\text{III}}\text{O}_3 + \text{Ti}^{\text{IV}}\text{O}_2 \rightarrow \text{Ti}_3^{10/3}\text{O}_5$ .

It is a redox reaction:  $\text{Ti}^{\text{IV}} + 2/3\text{e}^- \rightarrow \text{Ti}^{10/3}$  (reduction) and  $2\text{Ti}^{\text{III}} - 2/3\text{e}^- \rightarrow 2\text{Ti}^{10/3}$  (oxidation), that is,  $\text{TiO}_2$  is an oxidizing agent and  $\text{Ti}_2\text{O}_3$  is a reducing agent. Thus, the increase in sintering temperature and chemical activity of  $\text{TiO}_2$  nanoparticles leads to an increase in the percentage of the  $\text{Ti}_3\text{O}_5$  phase in the ceramic structure. The effect of conductivity and electromagnetic wave absorption is achieved by adjusting the properties of ceramics by thermodiffusion of ions of variable valence into it, and creating a second phase with increased conductivity. By quantitatively changing the ratio of BeO and titanium-containing phases, as well as by regulating the degree of non-stoichiometry of titanium oxides, when the oxidation degree changes in the series  $\text{Ti}^{4+} \rightarrow \text{Ti}^{3+} \rightarrow \text{Ti}^{2+}$ , it is possible to effectively control the properties of such ceramics.

Commercially produced absorption ceramics has a composition of 70 wt.% BeO + 30 wt.%  $\text{TiO}_2$ , sintered at a temperature of 1520–1530 °C (sample P0). The results of the study of the microstructure of ceramics made of BeO– $\text{TiO}_2$  micropowders indicate that such ceramics is a two-phase mechanical mixture, where the white color represents the  $\text{TiO}_2$  phase and the dark color represents the BeO phase, as shown in Figure 2a,b.

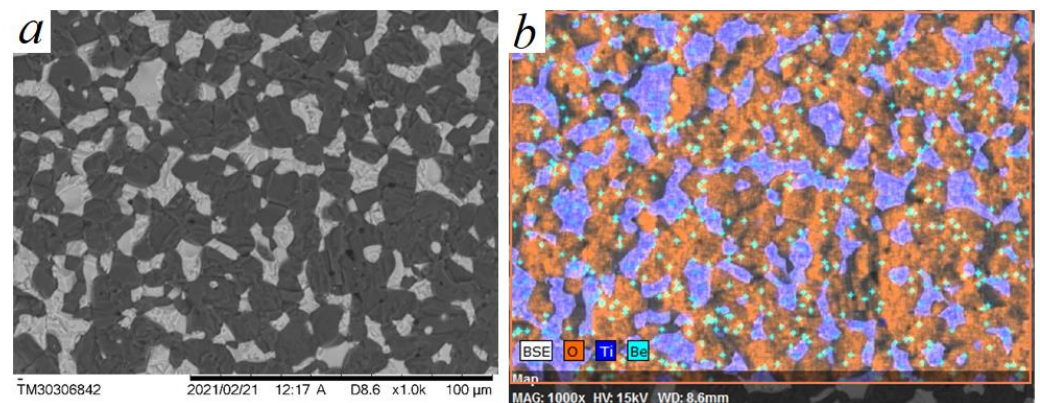


**Figure 2.** Microstructure of the ceramic sample of composition: BeO + 30% $\text{TiO}_2$ , obtained from micropowders of BeO and  $\text{TiO}_2$ , sintering temperature  $T = 1530$  °C, P0 composition sample. (a) SEM image of the microstructure of (BeO +  $\text{TiO}_2$ ) ceramics; (b) results of microanalysis of structural components of (BeO +  $\text{TiO}_2$ ) ceramics.

The temperature of solid-phase sintering of pure BeO ceramics in vacuum is 1920–1950 °C. Such ceramics has a density of 2.5–2.9  $\text{g}/\text{cm}^3$ ; the average grain size is 20–40  $\mu\text{m}$  [37] and has a dense structure with uniformly distributed grains, as shown in Figure 3a.

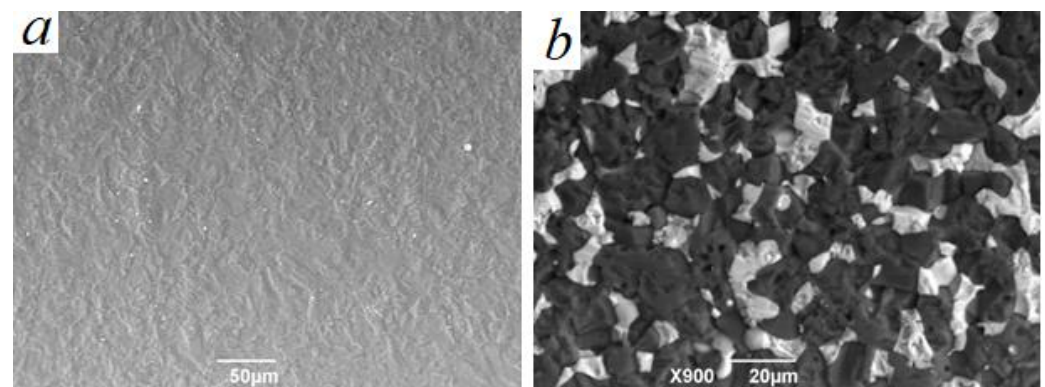


**Figure 3.** Microstructure of pure BeO ceramics and ceramics consisting of BeO and  $\text{TiO}_2$  micropowders, P0 composition sample: (a) SEM image of microstructure of BeO ceramics without impurities; (b) SEM image of microstructure of serial (BeO +  $\text{TiO}_2$ ) ceramics consisting of micropowders.

In the microstructure of (BeO + TiO<sub>2</sub>) ceramics made of P0 micropowders, as shown in Figure 3b at  $\times 900$  magnification, a rather porous and friable structure of the BeO phase is observed, which indicates that the temperature is not sufficient for the beginning of solid-phase sintering processes. In solid-phase sintering, the free energy changes with the change in the surface area of the crystal, and with the replacement of the solid–gas interface with the solid–solid interface [38]. Increasing the sintering temperature of serial ceramics consisting only of micropowders leads to the fact that the sample swells and loses density which affects geometric parameters, and the growth of TiO<sub>2</sub> grains occurs.

The introduction of TiO<sub>2</sub> nanoparticles in the composition of (BeO + TiO<sub>2</sub>) ceramics in the range from 0.5 to 1.5 wt.%, (Table 1) allows the sintering temperature of ceramics to increase by 130 °C. Thus, nanoparticles in the composition of ceramics contribute to restraining the growth of micron crystals of BeO and TiO<sub>2</sub> under the action of surface and bulk diffusion processes. The microstructure of such ceramics is presented in Figure 4.

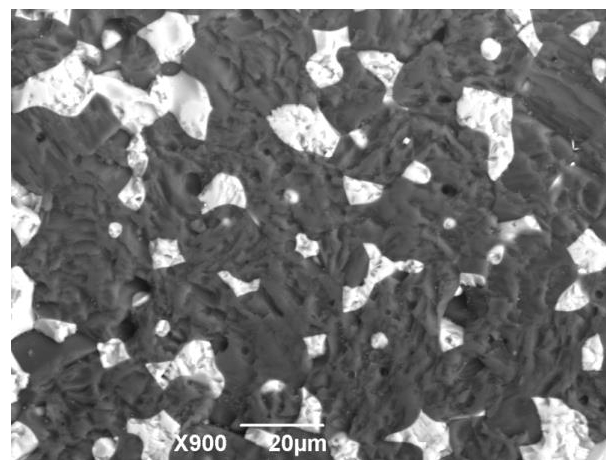


**Figure 4.** SEM image of microstructure of ceramics with nanoparticles addition of 1.0 wt.%, sintering temperature  $T = 1660$  °C, P2 composition sample.

Ceramics with the addition of nanoparticles has a denser structure; the intergranular boundaries between TiO<sub>2</sub> and BeO are reduced, and TiO<sub>2</sub> grains have an irregular shape as they penetrate into the intergranular spaces of BeO through better wetting and shrinkage of ceramics during sintering. The introduction of TiO<sub>2</sub> nanoparticles changes the mechanisms of mass transfer and microstructure formation. Changes in the mechanisms of surface diffusion and the mobility of TiO<sub>2</sub> across the interfacial grain boundaries lead to the formation of zonal shell structure elements, as shown in Figure 5a–c.

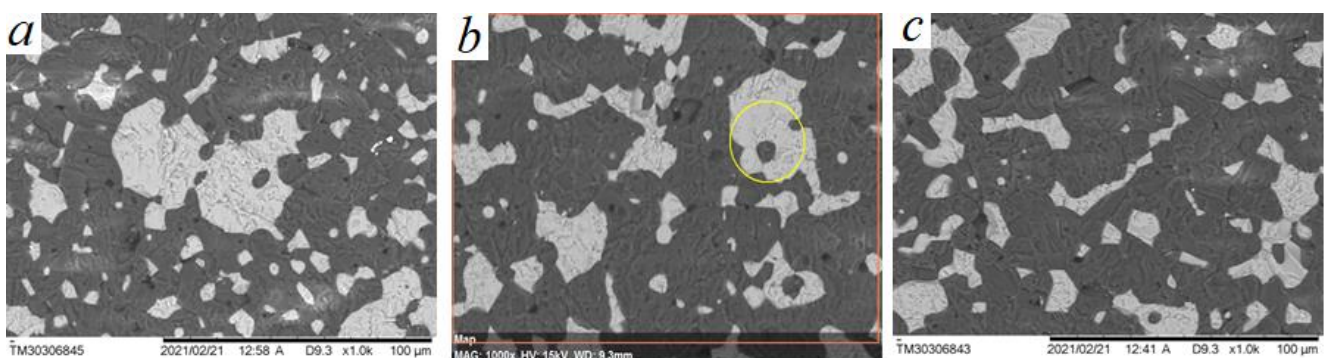


**Figure 5.** SEM image of the microstructure of ceramics with TiO<sub>2</sub> nanoparticles, sintering temperature  $T = 1660$  °C: (a) P1; (b) P2; (c) P3.

Thus, electron microscopy revealed the existence of  $\text{TiO}_2$  solid phase and liquid solution spreading at a certain temperature on the surface of  $\text{BeO}$  microcrystals, likely representing a mixture of oxides as components of the solution  $\text{Ti}_4\text{O}_7 + \text{TiO} + \text{Ti}_3\text{O}_5 + \text{Ti}_2\text{O}_3$ . Thus, the condensed medium formed by heating  $\text{TiO}_2$  in a reducing atmosphere is not only the initial  $\text{TiO}_2$  oxide in solid or liquid states.

The results of the chemical microanalysis interpretation of the shell structure fragment, as shown in Figure 5b (highlighted with a circle), are presented in Figure 6.

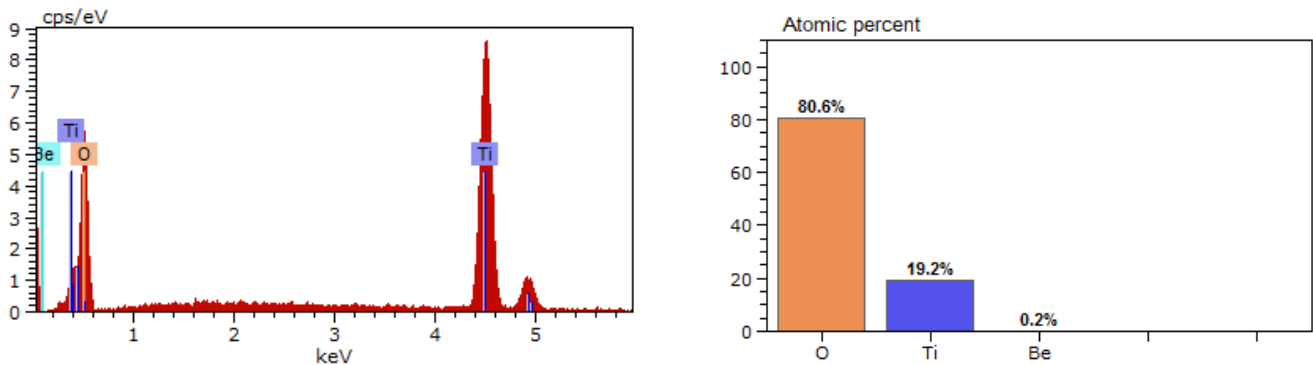


**Figure 6.** Chemical microanalysis of the element of the zone shell structure.

As it is known [39] to create capacitor segmental ceramics characterized by increased temperature stability  $\epsilon$ , mixtures of two phases of barium titanate are used. The second phase is a solid solution of heterovalent substitution of barium titanate with additives of simple or complex oxides. The grains of such ceramics have a zonal shell structure: each grain consists of a central part, barium titanate, and a shell–solid solution. The fact that the heterogeneous system is realized within a single grain ensures small changes in  $\epsilon$  over a wide temperature range.

The combination of these factors leads to the formation and development of interparticle boundaries and, consequently, to an increase in the density, hardness, and mechanical strength of the synthesized material, as shown in Table 3.

**Table 3.** Physical and mechanical properties of synthesized ceramics.

No. of Batch	Mechanical Strength, MPa	Microhardness, GPa	Density, g/cm <sup>3</sup>	Total Porosity, %
P0	280	9.3	3.22	7.1
P1	295	9.7	3.23	5.9
P2	300	10.0	3.24	5.3
P3	300	10.0	3.24	5.3

$\text{TiO}_2$  nanoparticles in the sintering process of ( $\text{BeO} + \text{TiO}_2$ ) ceramics promote the formation of  $\text{Ti}_3\text{O}_5$  phase due to the increased chemical activity and decrease in the interaction temperature during the reaction  $\text{Ti}_2\text{O}_3 + \text{TiO}_2 \rightarrow \text{Ti}_3\text{O}_5$ . In turn, the presence of  $\text{TiO}_2$  nanoparticles can increase the sintering temperature of ceramics. The growth of micron crystals of  $\text{BeO}$  and  $\text{TiO}_2$  is restrained under the action of mass transfer, surface and bulk diffusion processes. As a result, it was possible to obtain samples with increased density, while maintaining a homogeneous fine-grained structure with a 1–5  $\mu\text{m}$  grain size of  $\text{TiO}_2$ .

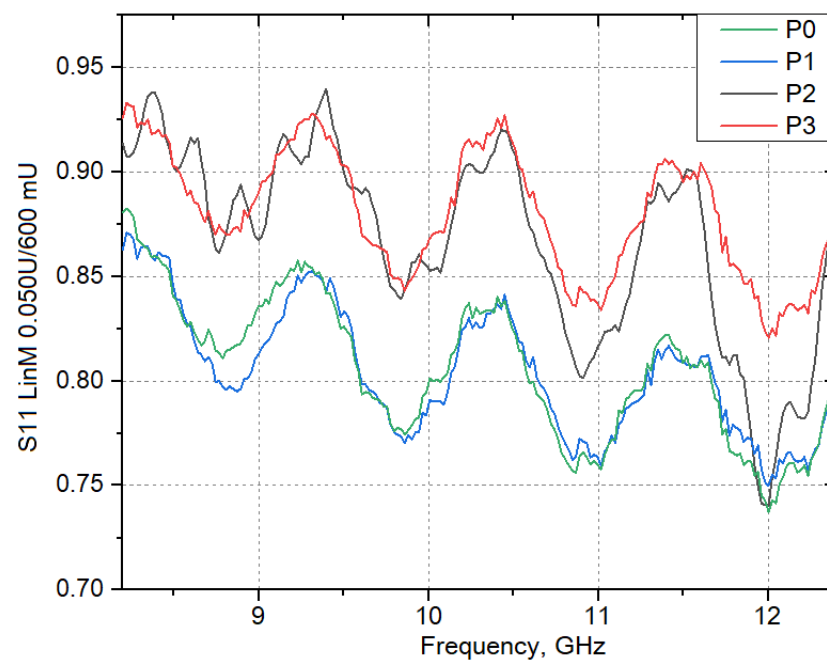
The main physical and mechanical characteristics of ceramics consisting of micropowders and ceramics modified with  $\text{TiO}_2$  nanoparticles are shown in Table 4.

**Table 4.** Properties of ceramics modified with TiO<sub>2</sub> nanoparticles in comparison with the sample consisting only of micropowders.

Parameter	BeO+30%TiO <sub>2</sub> <sup>μm</sup>	BeO+28.5%TiO <sub>2</sub> <sup>μm</sup> +1.5%TiO <sub>2</sub> <sup>nano</sup>
Number of grains with the size of 1–5 microns on the area of 0.137 mm <sup>2</sup> , pcs.	334	1257
Apparent density, g/cm <sup>3</sup>	3.2	3.24
Hardness, GPa	9.3	9.6
Mechanical strength, MPa	280	300

In addition, TiO<sub>2</sub> nanoparticles have a strong influence on crystallization processes, changing the rate of formation and growth of new phases, size distribution, and shape of crystals. The high value of specific surface area of powders consisting of TiO<sub>2</sub> nanoparticles can increase the diffusion rate and the rate of reduction reactions.

Next, the reflection coefficient (S11/S22 Lin Mag), the ratio of the complex amplitude of the reflected wave current to the complex amplitude of the incident wave current, was investigated on the “Vector network analyzer P9373A” in the frequency range of 8.2–12.4 GHz. The results are shown in Figure 7.

**Figure 7.** Variation of reflection coefficient (S11/S22 Lin Mag) in the frequency range of 8.2–12.4 GHz, depending on the concentration of TiO<sub>2</sub> nanoparticles.

As shown in Figure 7, the reflection coefficient of ceramics without TiO<sub>2</sub> nanoparticles addition at 8.2 GHz is the value of 0.88, then there is a monotonic sinusoidal decrease in the coefficient with the increase of electric current frequency. The first peak of 0.86 is observed at 9.3 GHz, the next peak of 0.84 at 10.3 GHz, then 0.82 at 11.4 GHz. At the introduction of TiO<sub>2</sub> nanoparticles in the amount of 0.5 wt.%, the curve of dependence of the reflection coefficient on the frequency of electric current practically matches the curve for the P0 sample. It should be noted that in the microstructure of sample P1, only single fragments of zonal shell structure are observed, which apparently makes the greatest contribution to the loss of electromagnetic radiation. At the content of TiO<sub>2</sub> nanoparticles—1.0 wt.% there is a sharp jump in the values of the reflection coefficient from 0.85 to 0.95 at a frequency of 8.2 GHz. With the increasing frequency of the electric current, the reflection coefficient also changes along a sinusoid with increasing amplitude. At the content of

TiO<sub>2</sub> particles—1.5 wt.% there is not a large increase in peak values, and the amplitude of reflection coefficient oscillation decreases.

The occurring changes in adsorption properties can be explained by the fact that titanium ions in the process of heat treatment of (BeO + TiO<sub>2</sub>)-ceramics are in bi-, tri-, and quadrivalent states. This promotes the occurrence of electron exchange between the localized states of Ti<sup>2+</sup> ↔ Ti<sup>3+</sup> ↔ Ti<sup>4+</sup> ions. As is already known, in the Ti–O system the main condensed phases are five oxides, the most refractory of which is TiO<sub>2</sub> with a melting point of 1912 °C. For the other oxides it is 1837 °C (Ti<sub>2</sub>O<sub>3</sub>), 1777 °C (Ti<sub>3</sub>O<sub>5</sub>), 1757 °C (TiO), and 1687 °C (Ti<sub>4</sub>O<sub>7</sub>). During sintering at 1660 °C in (BeO + TiO<sub>2</sub>) ceramics with the addition of TiO<sub>2</sub> nanoparticles, the melting point of refractory oxides decreases. The obtained diffractograms of the studied samples, as shown in Figure 8, indicate a high degree of structural ordering and a more efficient transformation of the crystalline structure of TiO<sub>2</sub> compound into an electrically conductive Ti<sub>3</sub>O<sub>5</sub> compound.

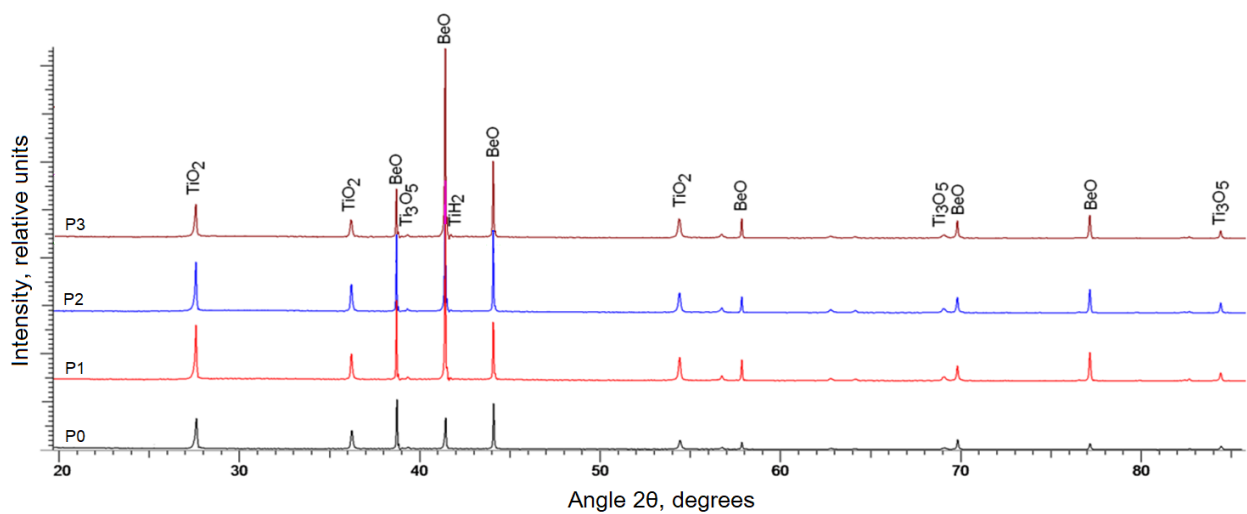


**Figure 8.** X-ray diffractograms of the studied ceramics. P0—serial sample, P1–P3—samples sintered at 1660 °C with different concentration of TiO<sub>2</sub> nanoparticles (0.5–1.5) wt.%.

The main contribution, according to the phase analysis in the structure of ceramics, corresponds to the phases of titanium dioxide (rutile) and beryllium oxide. Additionally, in the structure there are impurity inclusions characteristic for tetragonal TiH<sub>2</sub> and orthorhombic Ti<sub>3</sub>O<sub>5</sub> phases (Table 5), the content of which varies depending on the amount of introduced nano additives. The deviation of lattice parameters is associated with deformation processes occurring as a result of the formation of ceramics, as well as the presence of impurity phases and solid solutions of substitution and introduction.

**Table 5.** Phase composition and lattice parameters of synthesized ceramics in comparison with the serial sample.

Phase	Type of Structure	P0, Content%	P1, Content%	P2, Content%	P3, Content%
TiO <sub>2</sub> (rutile)	Tetragonal	49.0	41.3	39.8	40.4
BeO	Hexagonal	37.1	32.1	30.1	30.0
TiH <sub>2</sub>	Tetragonal	3.7	6.9	7.7	7.2
Ti <sub>3</sub> O <sub>5</sub>	Orthorhombic	10.2	19.7	22.4	22.4

Thus, the main chemical transformations occurring under conditions of high temperature synthesis of (BeO + TiO<sub>2</sub>) ceramics have been established, with the addition of TiO<sub>2</sub> nanoparticles during heating in a reducing atmosphere. The X-ray phase method shows that in the samples of (BeO + TiO<sub>2</sub>) ceramics—along with reflexes from the crystalline structure of BeO, diffraction peaks of TiO<sub>2</sub> corresponding to the crystalline modifications of rutile and anatase, as well as the background in the region of small angles—some amounts of the amorphous phase are fixed. In addition, weak reflections that are likely corresponding to titanium carbide and other phases, but which could not be identified, were recorded.

The degree of TiO<sub>2</sub> reduction in BeO ceramics is related to the magnitude of dielectric losses. Deviation of TiO<sub>2</sub> from the stoichiometric composition leads to a strong change in its electrophysical properties. According to the results of the authors' studies [33–35], the main absorbing phase of microwave radiation is the semiconducting non-stoichiometric compound Ti<sub>3</sub>O<sub>5</sub>, formed by the reduction of TiO<sub>2</sub> dioxide during the thermal treatment of ceramics in a reducing medium.

#### 4. Conclusions

The main phases formed during sintering of (BeO + TiO<sub>2</sub>) ceramics in reducing medium—TiO, Ti<sub>2</sub>O<sub>3</sub>, Ti<sub>3</sub>O<sub>5</sub> and TiH—have been identified by the method of entropic calculation of equilibrium constants of chemical reactions. Introduction of TiO<sub>2</sub> nanoparticles in the composition of ceramics 70 wt.% BeO + 30 wt.% TiO<sub>2</sub> in the amount of 0.5–1.5 wt.% allows for the increase of the sintering temperature of such ceramics from 1530 to 1660 °C, which leads to changes in its microstructure and formation of fragments with the zonal shell structure. Thus, nanoparticles in the composition of (BeO + TiO<sub>2</sub>) ceramics contribute to restraining the growth of micron crystals of BeO and TiO<sub>2</sub> under the action of surface and bulk diffusion processes. The introduction of TiO<sub>2</sub> nanoparticles contributes to the densification of the ceramic structure due to the reduction of intergranular boundaries between TiO<sub>2</sub> and BeO, and it also revealed the existence of TiO<sub>2</sub> solid phase and liquid solution spreading at a certain temperature on the surface of BeO microcrystals.

The addition of TiO<sub>2</sub> nanoparticles to the composition of the studied ceramics leads to changes in mass transfer mechanisms for micro- and nanoparticles, which allows for synthesizing a material with increased density, hardness, and mechanical strength.

According to the results of studies on the frequency dependence of the reflection coefficient on the content of TiO<sub>2</sub> nanoparticles, it was found that the introduction of nanoparticles in the amount of 1.0–1.5 wt.%, and an increase in the sintering temperature of ceramics, leads to an increase in the ability of the material to absorb electromagnetic radiation in the frequency range of an electric current between 8.2–12.4 GHz.

Using the XRD method, it has been established that at sintering (BeO + TiO<sub>2</sub>) ceramics with nanoparticles addition in a vacuum and a weakly reducing medium CO, in the furnace atmosphere conditions of oxygen deficiency are created, at which the reaction  $2\text{TiO}_2 + \text{C} \rightarrow \text{Ti}_2\text{O}_3 + \text{CO}$  is preferable. In turn, when Ti<sub>2</sub>O<sub>3</sub> is fused with TiO<sub>2</sub> under the influence of temperature it forms a phase Ti<sub>3</sub>O<sub>5</sub>, which is a double oxide of tri- and tetravalent titanium  $\text{Ti}_2^{\text{III}}\text{O}_3 + \text{Ti}^{\text{IV}}\text{O}_2 \rightarrow \text{Ti}_3^{10/3}\text{O}_5$ . Thus, the increase in sintering temperature and chemical activity of TiO<sub>2</sub> nanoparticles leads to an increase in the content of the Ti<sub>3</sub>O<sub>5</sub> phase, and consequently, to an increase in the ability of the material to absorb electromagnetic radiation. Thus, quantitative change in the ratio of BeO and titanium-containing phases, as well as regulation of the particle size distribution and degree of non-stoichiometry of titanium oxides, allows us to effectively control the electrophysical properties of synthesized ceramics.

**Author Contributions:** A.P. and Z.S. designed the experiments; N.M., Z.T. and S.G. performed the experiments; A.P. and A.Z. analyzed the data; A.P., Z.S., A.Z. and N.M. wrote, reviewed and edited the paper. All authors have read and agreed to the published version of the manuscript.

**Funding:** This research was funded by the Science Committee of the Ministry of Education and Science of the Republic of Kazakhstan (Grant No. AP09058686).

**Institutional Review Board Statement:** Not applicable.

**Informed Consent Statement:** Not applicable.

**Data Availability Statement:** Not applicable.

**Conflicts of Interest:** The authors declare no conflict of interest.

## References

1. Green, M.; Chen, X. Recent Progress of Nanomaterials for Microwave Absorption. *J. Mater.* **2019**, *5*, 503–541. [[CrossRef](#)]
2. Kiiko, V.S.; Pavlov, A.V. Composite (BeO + TiO<sub>2</sub>)-Ceramic for Electronic Engineering and Other Fields of Technology (Review). *Refract. Ind. Ceram* **2018**, *58*, 687–692. [[CrossRef](#)]
3. Akishin, G.P.; Turnaev, S.K.; Vaispapis, V.Y.; Gorbunova, M.A.; Makurin, Y.N.; Kiiko, V.S.; Ivanovskii, A.L. Thermal Conductivity of Beryllium Oxide Ceramic. *Refract. Ind. Ceram* **2009**, *50*, 465–468. [[CrossRef](#)]
4. Li, P.W.; Wang, C.B.; Liu, H.X.; Shen, Q.; Zhang, L.M. Structural, Thermal and Dielectric Properties of AlN–SiC Composites Fabricated by Plasma Activated Sintering. *Adv. Appl. Ceram.* **2019**, *118*, 313–320. [[CrossRef](#)]
5. Kiiko, V.S.; Makurin, Y.N.; Ivanovsky, A.L. Ceramics Based on Beryllium Oxide: Preparation, Physical and Chemical Properties and Application. Monography. *Ekaterinburg UrO RAS* **2006**, *440*, 2. (In Russian)
6. Kiiko, V.S.; Shabunin, S.N.; Makurin, Y.N. Fabrication, Physicochemical Properties, and Transmission of UHF Radiation by a BeO Ceramic. *Ogneup. Tekh. Keram* **2004**, 8–17.
7. Belyaev, R.A. Beryllium Oxide. *Mosc. At.* **1980**, *224*, 1. (In Russian)
8. Weispapir, V.Y.; Kiyko, V.S. Beryllium Ceramics for Modern Areas of Technology. *Bull. Air Space Def.* **2018**, 59–69. (In Russian)
9. Zdorovets, M.V.; Kozlovskiy, A.L.; Borgekov, D.B.; Shlimas, D.I. Study of Change in Beryllium Oxide Strength Properties as a Result of Irradiation with Heavy Ions. *Eurasian J. Phys. Funct. Mater.* **2021**, *5*, 192–199. [[CrossRef](#)]
10. Kiiko, V.S. Transparent Beryllia Ceramics for Laser Technology and Ionizing Radiation Dosimetry. *Refract. Ind. Ceram.* **2004**, *45*, 266–272. [[CrossRef](#)]
11. Akishin, G.P.; Turnaev, S.K.; Kiiko, V.S. Properties of Oxide Beryllium Ceramics. *New Refract.* **2010**, *10*, 42–47. (In Russian)
12. Ivanovsky, A.L.; Shein, I.R.; Makurin, Y.N.; Kiiko, V.S.; Gorbunova, M.A. Electronic Structure and Properties of Beryllium Oxide. *Inorg. Mater.* **2009**, *45*, 263–275. (In Russian) [[CrossRef](#)]
13. Drokin, N.A.; Kiiko, V.S.; Pavlov, A.V.; Malkin, A.I. BT-30 Ceramic Electrophysical Properties. *Refract. Ind. Ceram.* **2020**, *61*, 341–348. [[CrossRef](#)]
14. Ropp, R.C. *Encyclopedia of the Alkaline Earth Compounds*; Elsevier: Amsterdam, The Netherlands, 2012; ISBN 0-444-59553-8.
15. Kiiko, V.S.; Gorbunova, M.A.; Makurin, Y.N.; Neuimin, A.D.; Ivanovsky, A.L. Microstructure and electrical conductivity of composite (BeO + TiO<sub>2</sub>)-ceramics. *New Refract.* **2007**, 68–75. (In Russian)
16. Nazir, S.; Noor, N.A.; Afzal, Q.; Mahmood, A. Pressure-Induced Thermodynamic and Opto-Electronic Behavior of BeTiO<sub>3</sub> Perovskite: A DFT Investigation. *J. Electron. Mater.* **2020**, *49*, 3072–3079. [[CrossRef](#)]
17. Kiiko, V.S.; Gorbunova, M.A.; Makurin, Y.N.; Neuimin, A.D.; Ivanovskii, A.L. Microstructure and Electric Conductivity of Composite (BeO + TiO<sub>2</sub>) Ceramics. *Refract. Ind. Ceram.* **2007**, *48*, 429–434. [[CrossRef](#)]
18. Kiiko, V.S. Influence of Titanium Dioxide Additives on Physico-Chemical and Luminescent Properties of Beryllium Ceramics. *Inorg. Mater.* **1994**, *30*, 688–693. (In Russian)
19. Ivanovsky, A.L.; Kiiko, V.S.; Akishin, G.P.; Makurin, Y.N. Method of Obtaining Electrically Conductive Ceramics on the Basis of Beryllium Oxide. Patent 2326091 RU C2 C 04 B 35/08, 6 December 2008. (In Russian)
20. Rath, W. Ceramic special masses for electrical engineering. *Keram. Radsch.* **1941**, *49*, 137–179. (In German)
21. Kiiko, V.S.; Gorbunova, M.A.; Makurin, Y.N.; Ivanovsky, A.L. Development of Technology and Prospects of BeO Ceramics Application in New Areas of Technics and Special Instrumentation. *Constr. Compos. Mater.* **2006**, 98–100. (In Russian)
22. Mikhaylov, R.V.; Lisachenko, A.A.; Shelimov, B.N.; Kazansky, V.B.; Martra, G.; Alberto, G.; Coluccia, S. FTIR and TPD Analysis of Surface Species on a TiO<sub>2</sub> Photocatalyst Exposed to NO, CO, and NO-CO Mixtures: Effect of UV-Vis Light Irradiation. *J. Phys. Chem. C* **2009**, *113*, 20381–20387. [[CrossRef](#)]
23. Li, M.; Hebenstreit, W.; Diebold, U. Morphology Change of Oxygen-Restructured TiO<sub>2</sub> (110) Surfaces by UHV Annealing: Formation of a Low-Temperature (1 × 2) Structure. *Phys. Rev. B* **2000**, *61*, 4926. [[CrossRef](#)]
24. Sekiya, T.; Kamei, S.; Kurita, S. Luminescence of Anatase TiO<sub>2</sub> Single Crystals Annealed in Oxygen Atmosphere. *J. Lumin.* **2000**, *87*, 1140–1142. [[CrossRef](#)]
25. Di Valentin, C.; Pacchioni, G.; Selloni, A. Theory of Carbon Doping of Titanium Dioxide. *Chem. Mater.* **2005**, *17*, 6656–6665. [[CrossRef](#)]
26. Lira, E.; Hansen, J.Ø.; Huo, P.; Bechstein, R.; Galliker, P.; Lægsgaard, E.; Hammer, B.; Wendt, S.; Besenbacher, F. Dissociative and Molecular Oxygen Chemisorption Channels on Reduced Rutile TiO<sub>2</sub> (110): An STM and TPD Study. *Surf. Sci.* **2010**, *604*, 1945–1960. [[CrossRef](#)]
27. He, J.; Finnis, M.W.; Dickey, E.C.; Sinnott, S.B. Charged Defect Formation Energies in TiO<sub>2</sub> Using the Supercell Approximation. *Adv. Sci. Technol.* **2006**, *45*, 1–8.

28. Silvi, B.; Fourati, N.; Nada, R.; Catlow, C.R.A. Pseudopotential Periodic Hartree-Fock Study of Rutile TiO<sub>2</sub>. *J. Phys. Chem. Solids* **1991**, *52*, 1005–1009. [[CrossRef](#)]
29. Liao, L.-F.; Lien, C.-F.; Shieh, D.-L.; Chen, M.-T.; Lin, J.-L. FTIR Study of Adsorption and Photoassisted Oxygen Isotopic Exchange of Carbon Monoxide, Carbon Dioxide, Carbonate, and Formate on TiO<sub>2</sub>. *J. Phys. Chem. B* **2002**, *106*, 11240–11246. [[CrossRef](#)]
30. Yanagisawa, Y.; Ota, Y. Thermal and Photo-Stimulated Desorption of Chemisorbed Oxygen Molecules from Titanium Dioxide Surfaces. *Surf. Sci. Lett.* **1991**, *254*, 433–436.
31. Thompson, T.L.; Diwald, O.; Yates, J.T., Jr. Molecular Oxygen-Mediated Vacancy Diffusion on TiO<sub>2</sub> (1 1 0)-New Studies of the Proposed Mechanism. *Chem. Phys. Lett.* **2004**, *393*, 28–30. [[CrossRef](#)]
32. Green, D.S.; Dohrman, C.L.; Chang, T.-H. Compound Semiconductor Technology for Modern RF Modules: Status and Future Directions. *CS MANTECH* **2015**, 11–14.
33. Kiiko, V.S.; Pavlov, A.V.; Bykov, V.A. Production and Thermophysical Properties of BeO Ceramics with the Addition of Nanocrystalline Titanium Dioxide. *Refract. Ind. Ceram.* **2019**, *59*, 616–622. [[CrossRef](#)]
34. Malkin, A.; Korotkov, A.; Knyazev, N.; Kijko, V.; Pavlov, A. Approbation of the Measurement Method to Determining the Permittivity of Micro- and Nanopowders of Titanium Dioxide. In Proceedings of the 2019 International Multi-Conference on Engineering, Computer and Information Sciences (SIBIRCON), Novosibirsk, Russia, 21–22 October 2019; pp. 217–220.
35. Pavlov, A.V.; Lepeshev, A.A.; Rakhadilov, B.K.; Kantai, N. Method of obtaining electrically conductive ceramics based on beryllium oxide with the addition of titanium dioxide nanoparticles. KZ Utility Model Patent No. 34648, 23 October 2020. (In Russian)
36. Toropov, N.A. State diagrams of silicate systems. Reference book. *Leningr. Nauka* **1969**, *2*, 377. (In Russian)
37. Kascheev, I.D.; Strelov, K.K.; Mamykin, P.S. *Chemical Technology of Refractories. Textbook*; Intermet Engineering: Moscow Oblast, Russia, 2007; p. 752. (In Russian)
38. Mikhailov, M.D. Modern Problems of Materials Science. *Nanocompos. Mater.* **2010**, 67–70. (In Russian)
39. Khanin, S.D.; Ader, A.I.; Vorontsov, V.N.; Denisova, O.V.; Holkin, V.Y. Passive Radio Components. Part 1: Electrical Capacitors. *SPb. SZPI* **1998**, 28–30. (In Russian)

**Disclaimer/Publisher's Note:** The statements, opinions and data contained in all publications are solely those of the individual author(s) and contributor(s) and not of MDPI and/or the editor(s). MDPI and/or the editor(s) disclaim responsibility for any injury to people or property resulting from any ideas, methods, instructions or products referred to in the content.